Genome-wide analysis identifies genetic effects on reproductive success and ongoing natural selection at the FADS locus

Mathieson, I.; Day, F.R.; Barban, N.; Tropf, F.C.; Brazel, D.M.; Vaez, A.; ... ; Lifelines Cohort Study

Article

Genome-wide analysis identifies genetic effects on reproductive success and ongoing natural selection at the *FADS* locus

Check for updates

A list of authors and their affiliations appears at the end of the paper

Identifying genetic determinants of reproductive success may highlight mechanisms underlying fertility and identify alleles under present-day selection. Using data in 785,604 individuals of European ancestry, we identified 43 genomic loci associated with either number of children ever born (NEB) or childlessness. These loci span diverse aspects of reproductive biology, including puberty timing, age at first birth, sex hormone regulation, endometriosis and age at menopause. Missense variants in *ARHGAP27* were associated with higher NEB but shorter reproductive lifespan, suggesting a trade-off at this locus between reproductive ageing and intensity. Other genes implicated by coding variants include *PIK3IP1*, *ZFP82* and *LRP4*, and our results suggest a new role for the melanocortin 1 receptor (*MC1R*) in reproductive biology. As NEB is one component of evolutionary fitness, our identified associations indicate loci under present-day natural selection. Integration with data from historical selection scans highlighted an allele in the *FADS1/2* gene locus that has been under selection for thousands of years and remains so today. Collectively, our findings demonstrate that a broad range of biological mechanisms contribute to reproductive success.

Variation in human reproductive behaviour and success is epidemiologically associated with disease risk and has profound psychological, clinical and societal implications. This is particularly true for infertility, where efforts to elucidate the underlying biological mechanisms have been limited by the lack of large, well-phenotyped cohorts with relevant outcomes. This situation is mirrored across many reproductive traits and diseases, such as polycystic ovary syndrome[1,2], where progress in identifying genetic determinants and underlying mechanisms has lagged behind that of other complex diseases[3]. One reason for this is that natural selection limits the frequency of fertility-reducing alleles. The number of children ever born (NEB) to an individual has one of the highest degrees of polygenicity of any trait, consistent with a genetic architecture strongly influenced by negative selection[4,5]. Another reason is the fact that NEB is a behavioural phenotype influenced by multiple social, economic and environmental factors[6-8]. Nonetheless, studying the genetic basis of fertility may illuminate biological mechanisms underpinning infertility, with the advantage that the relevant measures are more readily available.

For example, recent studies have identified genetic determinants of NEB, age at first sexual intercourse and age at first birth[9-12]. These have provided several aetiological insights, such as highlighting a neuro-behavioural role for the oestrogen receptor in men[9] and identifying biological mechanisms linking reproductive ageing to late-onset diseases[9,10,13,14].

Fertility-associated loci may act through a broad array of mechanisms. They may have direct effects on reproductive biology or act through traits that contribute to partner selection or other aspects of behaviour and personality. For example, alleles associated with higher educational attainment are associated with lower fertility in some populations[15,16], reflecting the link between higher education and older age at childbearing[7]. Finally, fertility-associated loci might represent alleles under selection for some trait entirely disconnected from reproductive biology. By definition, any variant that is under natural selection affects fitness. Variants that affect fecundity would be detected by a genome-wide scan for NEB, although this scan would not capture all components of fitness.

✉e-mail: mathi@pennmedicine.upenn.edu; melinda.mills@nuffield.ox.ac.uk; john.perry@mrc-epid.cam.ac.uk

Our present study substantially builds on two earlier studies[9,10] to identify individual genetic determinants of NEB. In contrast to these previous studies, we double the sample size to 785,604 individuals and increase the number of genetic loci associated with NEB from 5 to 43. By linking our findings to scans for ancient selection, we isolate a unique example of an allele that has remained under selection for thousands of years and remains under selection today. We also highlight a number of biological mechanisms that contribute to reproductive success and uncover a previously unknown role for the melanocortin 1 receptor (*MC1R*) in reproductive biology.

Results

We identified genetic determinants of NEB by performing a genome-wide association study (GWAS) in 785,604 individuals of European ancestry meta-analysed across 45 studies (Supplementary Tables 1–6). The detailed methodology for how this discovery analysis was performed can be found in the Methods. Single nucleotide polymorphism (SNP) array data were imputed to at least the reference panel density of the 1000 Genomes Project (phase 1 version 3) across all studies. The distribution of genome-wide test statistics for NEB showed substantial inflation (λ_{GC} = 1.36); however, linkage disequilibrium (LD) score regression[17] indicated that this was attributable to polygenicity rather than population stratification (LD intercept, 1.01; s.e., 0.008). In total, 5,283 variants reached genome-wide significance ($P < 5 \times 10^{-8}$) for association with NEB, which we resolved to 28 statistically independent signals (Fig. 1 and Supplementary Table 7). These include all five signals previously reported for NEB in overlapping samples of up to 343,072 individuals[9,10].

The genetic architecture of NEB was only moderately correlated between men and women (r_g = 0.74; 95% confidence interval (CI), 0.66–0.82). We therefore ran separate GWAS meta-analyses in men (N = 306,980) and women (N = 478,624) and identified six additional statistically independent signals (two in men and four in women). We found evidence of heterogeneity ($P_{het} < 0.05$) between sexes at 13/34 NEB loci (greater than expected by chance; $P_{binomial} = 4 \times 10^{-9}$) and an overall trend for larger effect sizes in women than in men (24/34, $P_{binomial}$ = 0.02). Two notable examples were rs58117425 in the testis expressed 41 (*TEX41*) gene, which was significant only in men, and 6:152202621_GT_G in the oestrogen receptor alpha (*ESR1*), where the effect on NEB in women was double that in men (Supplementary Table 7). For all NEB-associated loci, we provide a summary of individual study effect estimates (Supplementary Table 8 and Supplementary Fig. 1).

In the absence of well-powered studies of infertility, we performed a GWAS on lifetime childlessness (CL) in UK Biobank (N = 450,082) and assessed the relevance of NEB-associated loci on susceptibility to CL. Effects on CL were modest, with the largest effect at the rs201815280-*CADM2* locus (sex-combined odds ratio, 1.05; 95% CI, 1.04 to 1.06; $P = 6.8 \times 10^{-18}$). Using LD score regression, we found that the genetic correlation between NEB and CL was very high but not perfect (r_g = −0.90; 95% CI, −0.88 to −0.92). Accordingly, of the 16 independent loci identified for CL, 8 were distinct from the NEB signals (Fig. 1 and Supplementary Table 7). Sex-stratified analyses revealed one additional female-specific CL signal (rs7580304, *PPP3R1*, Supplementary Table 7). Several loci exhibited significantly smaller or larger effects on CL than expected given their effect on NEB (Supplementary Fig. 2 and Supplementary Table 7).

In summary, we identified 43 independent signals comprising 28 from the sex-combined NEB meta-analysis, 6 sex-specific NEB signals, 8 additional sex-combined CL signals and 1 sex-specific CL locus. We did not identify any genome-wide significant signals on the X chromosome, probably due to a combination of chance and a slightly smaller discovery sample size (671,349 rather than 785,604 for autosomes). We note, however, that the heritability of all individual chromosomes—including the X chromosome—was broadly proportional to their size (Supplementary Fig. 3), suggesting that future expanded discovery efforts are likely to also identify signals there. To validate these findings, we examined associations of these signals in 34,367 women from the FinnGen study (Methods). Since NEB was not recorded for men in FinnGen, we considered only the 41 signals identified in sex-combined or female-specific analyses. Despite the small replication sample, 35 of 41 loci had the same direction of effect in FinnGen as in the discovery sample (binomial sign test, $P = 5 \times 10^{-6}$; Supplementary Table 7 and Supplementary Fig. 4).

Previous demographic research demonstrates that NEB is strongly influenced by socio-environmental factors such as education, employment uncertainty, religiosity, housing and larger trends such as economic and unemployment trends, policy measures (for example, childcare and taxes) and contraceptive technologies[6]. None of our identified signals exhibited genome-wide significant associations with educational attainment, church attendance or social deprivation indices (all of which have reported genetic associations[18,19]) (Supplementary Table 9). To investigate the possibility of subtle stratification, we explored the effect of increasing the number of principal components in the GWAS model from 10 to 40 in UK Biobank and found little change in the sizes of effect estimates at the 43 significant loci (average change, −0.6%; range, −8.7% to +12.7%; Supplementary Table 10). However, since this type of stratification can never be fully controlled, we turned to alternative sources of information to identify plausible mechanisms and candidate genes to prioritize the association signals more likely to be driven by biology than by stratification.

Implicated genes and biological mechanisms

We used a combination of in silico fine-mapping and summary-based Mendelian randomization (SMR) using expression quantitative trait loci (eQTL) data integration to identify putatively causal genes (Methods and Supplementary Table 7). Four of the 43 signals were highly correlated (pairwise r^2 = 0.9) with a non-synonymous variant, implicating *ARHGAP27* (rs12949256, p.Ala117Thr), *PIK3IP1* (rs2040533, p.Thr251Ser), *ZFP82* (rs17206365, p.Leu59Met) and *LRP4* (rs6485702, p.Ile1086Val). Of note, *PIK3IP1* encodes a negative regulator of the PI3K/Akt/mTOR pathway, which is an intracellular signalling pathway with well-established roles in cell cycle regulation. Oocyte-specific deletion of *Pten* in mice removes the inhibiting effect of the PI3K pathway on primordial follicle activation, leading to premature recruitment and exhaustion of the entire primordial follicle pool[20].

We extended the approach of implicating genes using predicted deleterious variants by performing MAGMA[21] multi-marker gene-burden analyses restricted to the same predicted deleterious variants (Supplementary Tables 11–13). This approach identified significant genes within three of our identified regions (Supplementary Table 7), notably the gene encoding the *MC1R* ($P = 1.6 \times 10^{-8}$). This was driven by 13 independent non-synonymous variants, none of which were individually genome-wide significant (Supplementary Table 14). *MC1R* is expressed on the surface of skin and hair melanocytes and produces the pigment melanin by binding α-melanocyte stimulating hormone. Genetic variation at *MC1R* accounts for ~73% of the heritability of red hair colour[22], including our lead non-coding variant in this region (rs8051733, Supplementary Table 7) and the rarer coding alleles included in the MAGMA test. The NEB effect at this locus appeared significantly stronger in women than in men (Supplementary Table 7). Three sensitivity analyses suggested that hair colour association was not responsible for the observed NEB effect (due to either population structure or mating preference). First, within women in the UK Biobank, the NEB effect remained significant when red-headed women were excluded from the analyses and showed a consistent direction of effect within women of the same hair colour (Supplementary Table 16). Furthermore, the inclusion of hair colour in the association model reduced the effect size by only 20–25% (Supplementary Table 15), suggesting that mating preference based on hair colour is unlikely to fully explain the observed effect. Second, there was
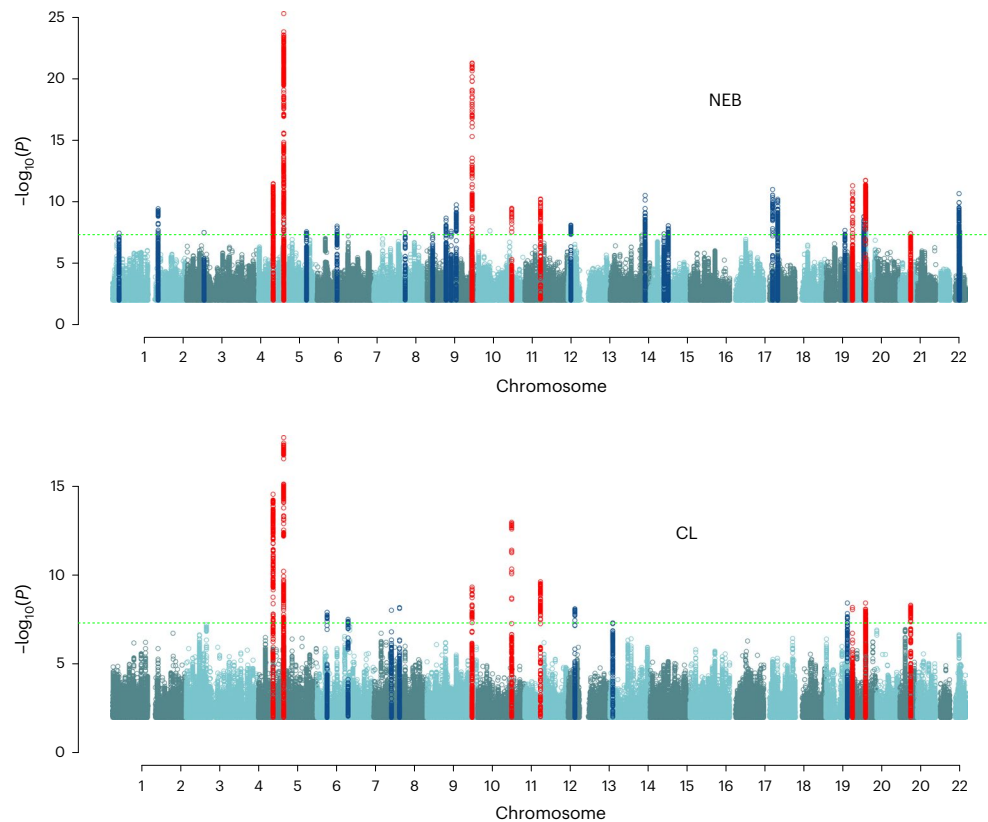
Fig. 1 | Manhattan plots for genome-wide association analyses of NEB and CL. The green dashed lines indicate the genome-wide significance threshold ($P = 5 \times 10^{-8}$, from a two-sided inverse-weighted meta-analysis in the case of NEB, and a two-sided BOLT infinitesimal model in the case of CL). Variants that fall within 300 kilobases (kb) of an identified signal are highlighted: those in blue are specific to either NEB or CL; those in red were significant for both. Only SNPs with a P value less than 0.01 are represented.

no concordance between individual SNP effects on hair colour and NEB (Supplementary Table 14). For example, the red-hair-increasing allele at Arg151Cys decreased NEB ($\beta = -0.02$; 95% CI, -0.03 to -0.01; $P = 1.3 \times 10^{-4}$), while the red-hair-increasing allele at Val92Met increased NEB ($\beta = 0.016$; 95% CI, 0.004 to 0.028, $P = 3.9 \times 10^{-3}$). Finally, we assessed the impact of *MC1R* loss of function using exome sequence data in ~450,000 UK Biobank participants. The 1,511 carriers of *MC1R* loss-of-function alleles showed no difference in NEB ($\beta = 0.01$; 95% CI, -0.04 to 0.07; $P = 0.65$), but these loss-of-function alleles had a very robust effect on the presence of red hair ($P = 1.8 \times 10^{-792}$), suggesting an alternative mechanism. Collectively, these data suggest a new role of the *MC1R* in reproduction, consistent with the recent observations that other pigmentation genes are associated with puberty timing in males[23].

MAGMA also highlighted three genes outside regions identified by the 43 loci: *ATHL1* (6 variants), *GLDN* (11 variants) and *RPS11* (2 variants). The association at *RPS11* was primarily driven by a single rare variant (rs739346, p.Thr77Ser), which had a relatively large effect on NEB ('T' allele frequency, 0.13%; $\beta = 0.18$; 95% CI, 0.11 to 0.25; $P = 9.7 \times 10^{-9}$). This gene encodes a key component of the complex that forms the ribosome and is one of the most differentially expressed genes in the sperm of men with asthenozoospermia[24].

Next, we systematically integrated publicly available gene expression QTL data with our GWAS meta-analysis results (Methods). To guide these analyses, we first assessed the relative genome-wide enrichment of NEB-associated variants near genes expressed in 53 GTEx cell types. In sex-combined analyses, a number of neuronal cell types reached significance (Supplementary Table 17). This pattern of enrichment is consistent with other reproductive traits such

as puberty timing[13], probably reflecting the established role of genes in the hypothalamic–pituitary–gonadal axis regulating fertility and reproductive ageing. Sex-stratified analyses demonstrated a similar enrichment while also highlighting genes expressed in the testis for men (Supplementary Table 17). Focusing on genes expressed in the brain, gonads and blood, SMR analyses suggest that 7 of our 43 genetic variants influence NEB through the expression levels of one or more nearby genes (Supplementary Table 7). This includes *IKZF3*, which encodes a haematopoietic-specific transcription factor involved in B-cell differentiation and proliferation, where correlated variants were recently reportedly associated with mosaic Y chromosome loss[25].

While we were unable to putatively link all our significantly associated genetic variants to gene function, we note that many are in or near genes with established links to aspects of reproductive biology (Supplementary Tables 7 and 18). This includes genes such as oestrogen receptor 1 (*ESR1*); *ENO4*, which is required for sperm motility and function as well as for male fertility in mice[26]; and *WNT4*, which encodes a regulator of Müllerian-duct formation and control of ovarian steroidogenesis. This signal in *WNT4* is the same as that previously reported for both uterine fibroids and endometriosis, with the disease-risk-increasing allele associated with lower NEB in women but not in men (Supplementary Table 7; $\beta_{all} = -0.01$; 95% CI$_{all}$, -0.02 to -0.01; $P_{all} = 3.6 \times 10^{-8}$; $\beta_{women} = -0.01$; 95% CI$_{women}$, -0.02 to -0.01; $P_{women} = 4.5 \times 10^{-7}$; $\beta_{men} = -0.004$; 95% CI$_{men}$, -0.011 to 0.002; $P_{men} = 0.19$). We note that many of the gene-mapping approaches described above may identify multiple genes at individual loci, highlighting the challenges of moving from variant to gene function in complex trait genetics. Further experimental work will be required to fully elucidate which genes our identified signals implicate.
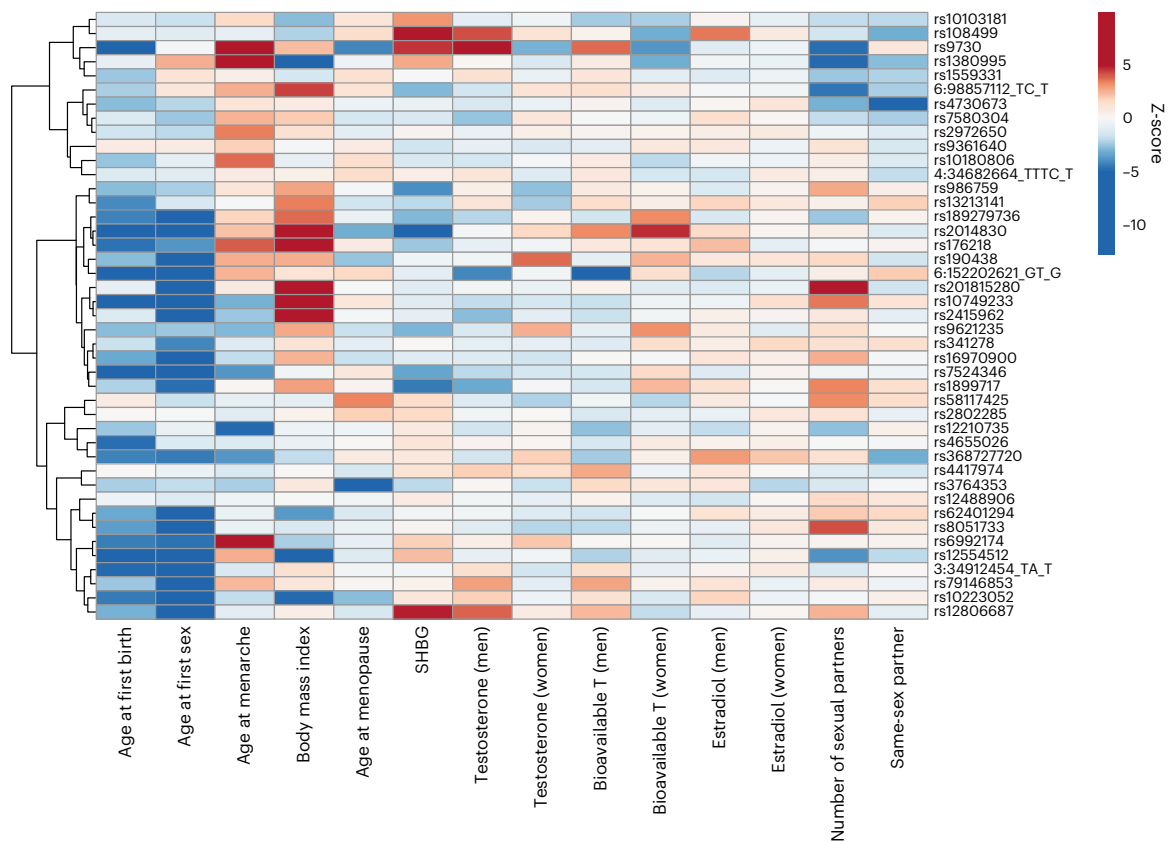
Fig. 2 | Heat map of the effects of the 43 independent signals identified for NEB or CL on other reproductive traits. All associations are based on trait-specific Z scores aligned to NEB-increasing alleles, with 0 (white) denoting no association, red colours representing positive associations, and blue negative associations. SHBG, sex hormone binding globulin; bioavailable T, bioavailable testosterone.

To further ascertain which loci might act directly on reproductive pathways, we integrated GWAS results from other reproductive traits (Fig. 2). We confirm previously reported systematic correlations between NEB and age at first birth, and between NEB and age at first sex[10,11]. However, other associations are less consistent. For example, a missense allele (rs9730, $r^2 = 1$ with rs12949256 / p.Ala117Thr) in *ARHGAP27*, which encodes a Rho GTPase (a small family of molecules involved in axon guidance), was associated with increased NEB but shorter reproductive lifespan—later age at menarche ($\beta = 0.04$ years; 95% CI, 0.03 to 0.05; $P = 1 \times 10^{-11}$) and earlier menopause ($\beta = -0.09$ years, 95% CI, −0.13 to −0.04; $P = 3 \times 10^{-5}$)—and with earlier age at first birth ($\beta = -0.07$ years; 95% CI, −0.09 to −0.04; $P = 5.5 \times 10^{-8}$), lower circulating testosterone concentrations in women (both bioavailable ($\beta = -0.01 \ln(\text{nmol l}^{-1})$; 95% CI, −0.02 to −0.01; $P = 2.1 \times 10^{-4}$) and total ($\beta = -0.011$ normalized units; 95% CI, −0.018 to −0.004; $P = 2.1 \times 10^{-3}$)), and higher testosterone concentrations in men (both bioavailable ($\beta = 0.01$ normalized units; 95% CI, 0.01 to 0.02; $P = 3.5 \times 10^{-4}$) and total ($\beta = 0.03$ normalized units; 95% CI, 0.02 to 0.03; $P = 1.9 \times 10^{-11}$)). Another NEB signal, rs4730673 near *MDFIC*, is correlated with the most significantly associated GWAS signal reported for same-sex sexual behaviour[27] (rs10261857; $r^2 = 0.74$). At this locus, the NEB-increasing allele was associated with a lower likelihood of same-sex sexual behaviour.

Overlap between NEB and historical selection identifies the *FADS* locus

Another approach to prioritize the most likely associations is to search for variants that show evidence of natural selection—that is, they also affected fitness in ancient populations. Effect estimates for the 34 genome-wide significant NEB loci ranged from 0.012 to 0.025 children per allele. The population mean NEB is ~1.8 in UK Biobank; thus, an

effect size of 0.02 per allele implies that a group of 25 people homozygous for an NEB-increasing allele would have, on average, 46 children, compared with 45 children for a group of 25 people without that allele. Assuming no effect on pre-reproductive mortality, these effect sizes can be directly translated to selection coefficients of 0.67–1.4% per allele, which is within the range detectable by genome-wide historical selection scans[28–30]. Accordingly, we compared our NEB/CL GWAS results with the results of scans testing selection over different timescales from ~2,000 to ~30,000 years before the present[28,29,31] (Methods) and evaluated overlap using Bayesian colocalization analysis[32] (Supplementary Tables 19 and 20).

The strongest overlap was observed at chr11:61.5 Mb, which exhibited a posterior probability of 96% that the lead variants for ancient selection and NEB represent the same underlying signal (Fig. 3a). This locus contains the genes *FADS1* and *FADS2*, which have been targeted by selection multiple times in human history[33–36]. In particular, the derived haplotype at this locus, which increases the expression of *FADS1*, has increased from a frequency of <10% 10,000 years ago to 60–75% in present-day European populations (Fig. 3b). While some of this increase is due to admixture, there is strong evidence of positive selection over the past few thousand years, even accounting for changes in ancestry[28,33–37]. *FADS1* and *FADS2* encode enzymes that catalyse the ω-3 and ω-6 lipid biosynthesis pathways that synthesize long-chain polyunsaturated fatty acids from short-chain precursors. It has been hypothesized that selection in Europe was driven by dietary transitions, in particular the Bronze Age transition to a diet based intensively on agricultural products with relatively low long-chain polyunsaturated fatty acid levels[36,37]. However, the mechanism through which this gene–environment interaction might affect fitness is unclear. Indeed, the *FADS* locus is highly pleiotropic. It is one of the strongest GWAS signals for
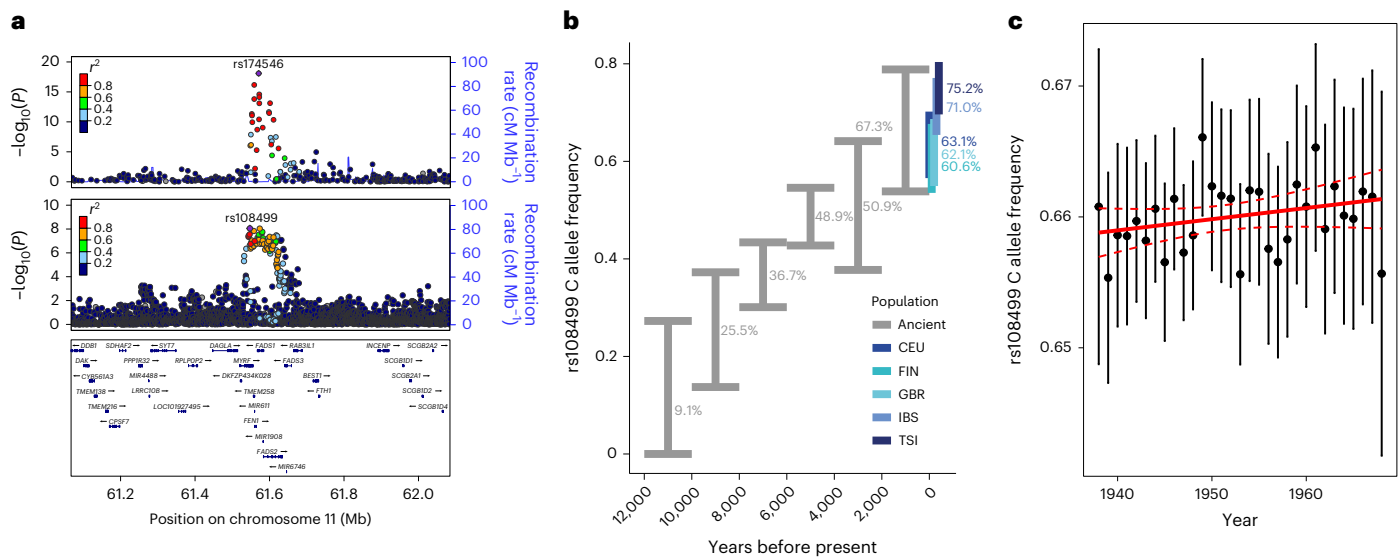
Fig. 3 | Evidence for historical and ongoing selection at the FADS locus.
a, Colocalization of the ancient DNA selection signal[28] (top) and the NEB GWAS signal (bottom). **b**, Estimated allele frequency (the error bars indicate the 95% CIs) for the derived *FADS* allele in Europe, based on direct evidence from 595 ancient DNA samples and 503 present-day samples. The present-day frequencies in 1000 Genomes European populations are shown in blue (CEU, Utah residents (CEPH) with Northern and Western European ancestry; FIN, Finnish in Finland; GBR, British in England and Scotland; IBS, Iberian population in Spain; TSI, Toscani in Italia). **c**, Allele frequency (the error bars indicate the 95% CIs) of the derived *FADS* allele in UK Biobank as a function of birth year from 1938 to 1968 using 274,318 individuals.

circulating lipids[38] and blood metabolites[39] and is strongly associated with blood cell phenotypes, including erythrocyte and platelet sizes and counts (Supplementary Table 21).

In our data, each 'C' allele of the lead NEB SNP rs108499, which tags the selected *FADS* haplotype, increased NEB by 0.0134 children, corresponding to a selection coefficient of 0.74% (0.0134 divided by the mean NEB of 1.8). Consistent with this, in the 'White British' subset of UK Biobank, the derived allele increased in frequency by 0.009% per year between the 1938 and 1969 birth cohorts (Fig. 3c), corresponding to a selection coefficient of 1.2% (95% CI, −0.9% to 3.2%). One caveat is that GWAS results can always be affected by stratification. To provide additional evidence, we turned to exome sequence data as an independent validation dataset. In UK Biobank exome sequence data, 242 *FADS1* loss-of-function carriers had lower NEB than non-carriers (Supplementary Table 22; $\beta = -0.21$; 95% CI, −0.35 to −0.06; $P = 5.3 \times 10^{-3}$). The NEB-increasing allele increases *FADS1* expression, so this effect is directionally consistent.

Further support for the association comes from three lines of evidence directly connecting *FADS1* to reproductive biology. First, the NEB-increasing allele is associated with higher circulating sex-hormone-binding globulin ($\beta = 0.009$ ln(nmol l^{-1}); 95% CI, 0.007 to 0.011; $P = 2.3 \times 10^{-20}$), total testosterone ($\beta = 0.013$ normalized units; 95% CI, 0.007 to 0.020; $P = 1.9 \times 10^{-5}$) and oestradiol concentrations ($\beta = 0.003$ normalized units; 95% CI, 0.001 to 0.005; $P = 4 \times 10^{-4}$) in men, and lower bioavailable testosterone concentrations in women ($\beta = -0.009$ ln(nmol l^{-1}); 95% CI, −0.014 to −0.003; $P = 1.5 \times 10^{-3}$). Second, *FADS1* is expressed in human oocytes and granulosa cells at various stages of development (Supplementary Table 23). Finally, in mice, knockout of *Fads2* (which acts in the same pathway) leads to infertility in both sexes, which can be rescued by dietary supplementation of long-chain polyunsaturated fatty acids[40]. In contrast, when we assessed the dose–response relationship of all previously reported[41] HDL, LDL, total cholesterol or triglyceride associated variants on NEB using a Mendelian randomization framework, we found no association ($P > 0.05$ in all models) with or without inclusion of the *FADS* locus. This suggests that the FADS locus does not affect NEB indirectly via these phenotypes. Ultimately, while further experimental work will be required to elucidate the mechanisms linking NEB-associated variants at this locus to reproductive success, our results support the association between *FADS1* variation and NEB.

NEB-associated genes exhibit signatures of balancing selection
The most significant NEB-associated variants in the genome, in *CADM2*, show no evidence of historical positive selection. However, *CADM2* is reported to exhibit one of the strongest genomic signals of long-term balancing selection[42]. Variants in *CADM2* are associated with a range of behavioural and reproductive traits, plausibly explained by a primary effect on risk-taking propensity[9,18,43]. Variants that increase risk taking also increase NEB, with risk taking and behavioural disinhibition also linked to earlier reproductive onset[11]. *ESR1*—the gene identified with our second-most-significant association—also contains signals of balancing selection[44], while other NEB-associated loci with nominal evidence of balancing selection contain the genes *PTPRD* and *LINC00871* (Supplementary Table 24). Balancing selection related to pleiotropy or time-varying or environmentally varying selection might explain why variants with relatively large effects on NEB are able to remain segregating in the population.

Lack of contemporary selection at historical selection signals
We next tested whether there was any evidence of ongoing selection (as measured by association with NEB or CL) at regions identified by the three genome-wide historical selection scans (Supplementary Table 25). Other than the *FADS* locus, none of the other 53 regions tested exhibited a significant association with NEB, suggesting that few of the strong historical selective sweeps in humans are ongoing. For example, the sweep associated with lactase persistence—one of the strongest signals of selection in any human population, stronger than that on FADS—could not be shown to be ongoing in the European-ancestry populations in this study. Other sweeps, such as those associated with skin-pigmentation-decreasing loci, are probably not detected in the NEB GWAS because the selected variants are now virtually fixed among European-ancestry populations.

Different methods for detecting selection in humans are sensitive to selection across very different timescales, ranging from thousands

to millions of years. Our GWAS can be interpreted as a genome-wide selection scan over the shortest timescale—living generations. The limited overlap between this and historical selection scans is consistent with the limited overlap among historical scans, reflecting a highly dynamic landscape of selection. Positively selected loci either fix or stop being selected due to changing environmental pressures and remain at intermediate frequencies. Balancing selection related to changing environments, or pleiotropic effects on other components of fitness, also helps maintain NEB-associated variants at intermediate frequencies. The *FADS* locus is unique in the sense that the selective sweep—starting at least several thousand years ago—is still ongoing.

In summary, our study identifies 38 signals that have not been previously reported for NEB and represent potential targets of ongoing natural selection. Further work should aim to parse these effects into mechanisms that directly influence reproductive biology, in contrast to those that affect behaviour or reduce fitness through premature morbidity or mortality. Finally, we note that our analysis includes only European-ancestry individuals and is heavily weighted by the UK Biobank, which is not representative of the UK population[45]. It remains to be seen which of these effects are consistent across cohorts and populations.

Methods

This study received ethical approval from the Department of Sociology, University of Oxford 2014/01/01/R3, on 28 January 2014 (SOCIOGENOME), revised with extension SOC/R2/001/C1A/21/60 on 7 July 2022 (CHRONO). Relevant ethical approval was obtained at the local level for the contributing datasets.

Phenotype definitions

NEB is treated as a continuous measure that was asked directly or could be created from several survey questions (for example, birth histories). A standard question in most surveys asks, 'How many children have you given birth to?' Another variant is 'How many children do you have?' In most cases, it was possible to distinguish between biological children, adopted children and step-children, and when this was possible, we refer to live-born biological children. Individuals were eligible for inclusion in the analysis if they were assessed for NEB and were at least age 45 for women and age 55 for men.

CL is a binary measure, derived from NEB, with a value of 1 for childlessness or 0 if an individual had children, with the same inclusion rules of biological live-born children and age restrictions that applied to NEB. Detailed measures for both phenotypes per cohort are described in Supplementary Table 2.

Participating cohorts and analysis plan

A total of 45 cohorts participated in our study (Supplementary Table 1). Supplementary Table 2 provides an overview of cohort-specific details, including an adjusted pooled analysis of women and men in the case of family data (see below). Cohorts who agreed to participate followed an Analysis Plan posted on the Open Science Framework preregistration site https://osf.io/b4r4b/ on 8 February 2017.

Cohort-level data were quality-controlled and meta-analysed by two separate independent centres at the University of Oxford and the University of Cambridge. We followed the quality control (QC) protocol of the GIANT consortium's study of human height[46] and employed the software packages QCGWAS[47] and EasyQC[48], which allowed us to harmonize the files and identify possible sources of errors in the association results. This procedure entailed that diagnostic graphs and statistics were generated for each set of GWAS results. In the case where apparent errors could not be amended by stringent QC and correspondence with the local analyst of the respective cohort, cohorts were excluded from the meta-analysis. (See the section below for details on cohort inclusion and errors.)

For NEB, the total number of individuals in the pooled meta-analysis was 785,604. Not all cohorts provided data about the X chromosome (Supplementary Table 3), meaning that the X chromosome analysis included only 671,349 individuals. The CL analysis was restricted to UK Biobank, with 450,082 individuals for both the autosomal and X chromosomes.

Sample exclusion criteria

Individuals were eligible for inclusion if they met the following conditions:

(a) They were assessed for NEB when at least age 45 for women and 55 for men.
(b) All relevant covariates (such as year of birth) were available for the individual.
(c) They were successfully genotyped genome-wide (recommended individual genotyping rate >95%).
(d) They passed the cohort-specific standard QCs (for example, excluding individuals who are genetic outliers in the cohort).
(e) They were of European ancestry.

Genotyping and imputation

Supplementary Table 4 provides an overview of the cohort-specific details of the genotyping platform, pre-imputation QC filters applied to the genotype data, the imputation software used, the reference panel used for imputation and the presence of X chromosome data. We asked the cohorts to include all autosomal SNPs imputed from the 1000 Genomes panel (at a minimum) to allow analyses across different genotyping platforms. Cohorts with denser reference panels were asked to communicate this to our team. Cohorts were asked to provide unfiltered results since filters on imputed markers were applied at the meta-analysis stage.

Association testing models

Analysts ran linear regression models for NEB and logistic regression models for CL. The analysts were asked to include the birth year of the respondent (represented by birth year minus 1900) and its square and cube to control for nonlinear birth cohort effects. For cohorts with family-based data, we suggested controlling for family structure or excluding relatives. Combined analyses that included both men and women included interactions of birth year and its polynomials with sex. We asked the cohorts to include the top principal components to control for population stratification[49] and cohort-specific covariates if appropriate. Some cohorts used only birth year and not the polynomials because of multi-collinearity issues or convergence of the GWA analysis. Per-chromosome heritability estimates were calculated using restricted maximum likelihood implemented in BOLT-LMM[50]. This analysis was performed for NEB in UK Biobank using directly genotyped variants in unrelated individuals of European ancestry.

X chromosome analysis

Analysis of X chromosome variants was performed using one of two approaches, XWAS or SNPtest, the results of which could be combined by meta-analysis. In XWAS software (http://keinanlab.cb.bscb.cornell.edu/content/xwas), we used the var-het-weight command. In SNPtest, we used the method newml. Since this assumes complete X inactivation (that is, a hemizygous male is considered the same as a homozygous female), the effect estimates and standard errors (s.e.) approximate ½ of those produced by XWAS.

Filters and diagnostic checks

We followed the QC protocol described by the GIANT consortium's GWAS of height[46]. We used an adapted version of the software package QCGWAS[47] (which allows the inclusion of structural variants) to standardize files across cohorts, and we used EasyQC[48] to filter variants by QC

criteria and to produce diagnostic graphs and statistics as described below. Where errors could not be amended by combining stringent QC with file inspections, queries to cohorts and corrections, cohorts were excluded from the meta-analysis. See also Supplementary Tables 5 and 6 for the QC results on autosomal and X chromosomes for NEB and CL. The specific individual filters were the following:

(a) Missing data. We filtered variants for which information on both reference and other alleles was missing or for which the estimated effect, P value, s.e., expected allele frequency or number of observations was missing.

(b) Implausible values. We filtered variants for which P values were >1 or <0, s.e. were 0 or infinite, expected allele frequencies were >1 or <0, N was <0, call rate was >1 or <0, an s.e. of the effect estimate was approximately 40% greater than the expected s.e. based on minor allele frequency (MAF) and standard deviation, or R^2 was >10% (see Winkler et al.[48] for the approximation for quantitative traits and Rietveld et al.[51] for quantitative and binary traits).

(c) Quality thresholds. We filtered variants for which the expected allele frequency was 1 or 0 (monomorphic variants), N was <100 (to guard against spurious associations due to overfitting of the model), the minor allele count was <6 (to guard against spurious associations with low-frequency SNPs and genotyped SNPs that were not in Hardy–Weinberg equilibrium, with significance thresholds of 10^{-3} if $N < 1,000$, 10^{-4} if $1,000 \leq N < 2,000$, 10^{-5} if $2,000 \leq N < 10,000$ and no filter if $N > 10,000$), imputed markers had an imputation quality <40% and SNPs had a call rate <95%, or discrepancies between the reported and expected P values based on effect estimates and s.e. were detected (see also the next section on diagnostic graphs).

(d) Data harmonization. We matched the cohort-based summary statistics with a 1000 Genomes phase 1 version 3 reference panel provided by Winkler et al.[48]. EasyQC drops mismatched variants that cannot be resolved, such as duplicates, allele mismatches or missing or invalid alleles. On the basis of graphical inspections (see below), we applied cohort-specific filters to drop variants with obvious deviations between the expected allele frequency based on the reference panel and the observed allele frequency.

Filtering results

Autosomal chromosomes. Overall, the quality of studies was good (for the full results of the QC filters described above, see Supplementary Tables 5 and 6 for autosomal SNPs). One cohort was excluded (INGI-Carlantino) due to the filter on sample size. For autosomal chromosomes and NEB, the remaining 45 cohorts provided 81 files: 39 for women only, 29 for men only and 13 pooled (from cohorts with family data). Two studies did not provide imputation quality (KORA F3, $N = 1,066$; and KORA F4, $N = 1,111$) and contributed only 584,866 and 496,556 SNPs respectively. For the two HPFS cohorts, the results from our last discovery GWAS[10] based on HapMap 2 reference panels were recycled with numbers of SNPs between 2,394,353 and 2,412,487. For all other cohorts, the number of variants in the analysis ranged between 6,691,978 for men in LBC 1921 and 20,783,286 for women in EPIC with an average of 10,574,721. For CL, between 25,555,939 and 25,554,098 variants from the UK Biobank entered the GWAS, and between 13,539,540 and 13,661,642 passed QC.

X chromosome. For NEB, 12 cohorts provided information on the X chromosome. Overall, we received 27 files: 12 for women, 10 for men and 5 for the pooled analysis if there were relatives in the data. On average, 325,872 variants passed QC, with a minimum of 191,880 in men from LBC 1921 and a maximum of 991,081 for the pooled UK Biobank sample. For CL, the UK Biobank provided results for between 980,779 and 991,081 variants on the X chromosome after QC.

GWAS meta-analysis and signal selection

Cohort association results (after applying the QC filters) were combined using sample-size weighted meta-analysis, implemented in METAL[52]. Sample-size weighting is based on Z scores and can account for different phenotypic measurements among cohorts[53]. The two QC centres agreed in using sample-size weighting to allow cohorts to introduce study-specific covariates in their cohort-level analysis. For each study, only SNPs that were observed in at least 50% of the participants for a given phenotype–sex combination were passed to the meta-analysis. SNPs were considered genome-wide significant at P values smaller than 5×10^{-8} (α of 5%, Bonferroni-corrected for one million tests). The meta-analyses were carried out by two independent analysts. Comparisons were made to ensure concordance of the identified signals between the two independent analysts. To identify independent signals, distance-based clumping (using a 1 Mb window) was used to identify the most significant SNPs in associated regions (termed 'lead SNPs'). This was then supplemented by approximate conditional analysis implemented in GCTA[54,55], where we required additional independent signals to be genome-wide significant in both pre and post conditional models.

We meta-analysed the GWAS results for NEB and CL in both sex-combined and sex-specific models. To understand the magnitude of the estimated effects, we used an approximation method to compute unstandardized regression coefficients based on the Z scores of METAL output obtained by sample-size-weighted meta-analysis, allele frequency and phenotype standard deviation. Supplementary Table 8 provides the forest plots of all genome-wide significant SNPs to provide a visualization of the effect size estimates for each cohort and the summary meta-analysis in addition to the 95% CIs. The genetic correlation between these two results was assessed using LD score regression[56].

Replication

Replication was performed using the FinnGen study—a public–private partnership project combining genotype data from Finnish biobanks and digital health record data from Finnish health registries (https://www.finngen.fi/en). Six regional and three country-wide Finnish biobanks participate in FinnGen, which also incorporates data from previously established populations and disease-based cohorts. Release 4 of FinnGen includes 176,899 participants.

In this analysis, we included women that participated in FinnGen release 4 and were at least 45 years of age by 31 December 2017. This was the last date for which we had information from national registries. We also excluded women younger than 16 in 1969 (the start of the registries). Using these inclusion criteria, we included women born between 1953 and 1973 and children born between 1969 and 2017. We also excluded women that emigrated from Finland in the study period.

To determine whether a woman delivered a child, we used the following codes obtained from the national inpatient registry (HILMO):

- ICD-10 codes: O80–O84
- ICD-9 codes: 6440B, 6450B, 650[0–9]B–659[0–9]B
- ICD-8 codes: 650–662

When multiple codes were used within a ten-month period, we counted it as a single delivery. There were 37,741 women, the average (s.d.) number of children was 1.72 (1.32) and 20.4% of the women were childless.

For principal components analysis, the FinnGen data were combined with the 1000 Genomes data. Related individuals (less than third degree) were removed using King software[57]. We considered common (MAF ≥ 0.05) high-quality variants: not in chromosome X, imputation INFO > 0.95, genotype imputed posterior probability > 0.95 and missingness < 0.01. LD-pruned ($r^2 < 0.1$) common variants were used for computing the principal components analysis with PLINK v.1.92 (ref. [58]). SAIGE mixed model logistic regression (https://github.com/weizhouUMICH/SAIGE/releases/tag/0.35.8.8) was used for association

analysis. Age, ten principal components and genotyping batch were used as covariates. Each genotyping batch was included as a covariate to avoid convergence issues.

Prioritizing and characterizing putatively functional genes in GWAS highlighted regions

We used three distinct approaches to identify putatively functional genes at each genome-wide significant locus. First, we assessed the coding impact of any variant in LD with our 43 lead index variants. We restricted our assessment to variants with $r^2 > 0.8$ and predicted moderate- or high-impact effects on the basis of Variant Effect Predictor (VEP) annotations. We calculated LD using PLINK v.1.9 from best-guess genotypes for 1000 Genomes Phase 3/HRC imputed variants in ~10,000 unrelated UK Biobank participants of white British ancestry. Second, we used MAGMA v.1.08 (ref. [21]) to collapse multiple predicted deleterious variants (using the same VEP categories above) into a single gene score. Finally, we integrated our genome-wide summary statistics with eQTL data using SMR[59]. Publicly available expression datasets for ovary and testis tissues in GTEx v.7, in addition to a meta-analysis of eQTL brain tissues, were downloaded from the SMR website (https://cnsgenomics.com/software/smr/#eQTLsummarydata). Whole-blood data in an eQTL meta-analysis of 31,684 samples was available from the eQTLGen consortium[60]. A Bonferroni-corrected P value threshold was used in each expression dataset individually, and only associations with HEIDI $P > 0.01$ were considered to avoid coincidental overlap due to extended patterns of LD. This resulted in a total of 11 (SMR $P < 6.6 \times 10^{-6}$) significant transcriptions in the brain, 12 in whole blood ($P < 3.2 \times 10^{-6}$) and 9 in the female-specific GTEx ovary analysis (SMR $P < 3.2 \times 10^{-5}$). We additionally performed tissue enrichment analysis using LD score regression to specifically expressed genes (LDSC–SEG)[61]. We used three datasets available on the LDSC–SEG resource page (https://github.com/bulik/ldsc/wiki/Cell-type-specific-analyses), relating to cell- and tissue-specific annotations from GTEx[62].

We characterized the phenotypic consequences of *MC1R*, *FADS1* and *FADS2* loss of function using up to 454,756 exome sequences in the UK Biobank study[63]. The exome-based association with variants in MC1R and hair colour was assessed with an interim release of 184,135 individuals. All variants were annotated using VEP, and we only considered those predicted to be high-impact loss of function defined by VEP. Individuals carrying one or more rare (MAF ≤ 0.1%) loss-of-function alleles in a given gene were grouped together. We created dummy variables on the basis of this definition for each gene and tested for association using BOLT-LMM[50].

All lookup data for additional traits were taken from previously described analyses. This includes sex hormones[64], number of sexual partners and same-sex behaviour[27], age at menarche and BMI[13], Townsend deprivation index[18], religious group attendance[18] and years of education[19].

Assessment of *FADS1-3* expression in human oocytes and granulosa cells at various stages of development

We used processed RNA-seq data on fetal primordial germ cells from two studies:

- Li et al.[65] (accession code: GSE86146) report data from 17 human female embryos ranging from 5 to 26 weeks post-fertilization.
- Zhang et al.[66] (accession code GSE107746) report data from follicles at five different stages of development from fresh ovarian tissue from seven adult donors, separated into oocytes and granulosa cell fractions.

We also generated new single-cell RNA-seq data from human MII oocytes. We performed sample QC and filtering of reads to remove low-quality reads, adaptor sequences and low-quality bases with Trimmomatic v.0.36 (ref. [67]) in two steps using ILLUMINACLIP:/ /Trimmomatic-0.36/adapters/NexteraPE-PE.fa:2:30:10

(SLIDINGWINDOW, 4, 20; CROP, 72; HEADCROP, 10; MINLEN, 40; followed by an extra trim of headbases with HEADCROP, 10). Subsequent to filtering, we used the remaining paired reads for alignment by hisat2 (ref. [68]) to the human genome GeneCode v.27 release with the paired GenCode v.27 GTF file containing gene annotations using: $HISAT2 -p 22 –dta -x.gencode.v27 -1 R1.fastq -2 R2.fastq -S sample.sam[69]. The resulting SAM files were sorted, indexed and transformed to BAM files using samtools[70]. QC measures of aligned reads were generated using Picard metrics (https://slowkow.github.io/picardmetrics) and the CollectRnaSeqMetrics tool from Picard tools (http://broadinstitute.github.io/picard). We filtered the BAM files for mitochondrial reads and applied Stringtie to merge and assemble reference guided transcripts for gene-level quantifications of raw counts, and transcripts per million[69]. Gene expression levels in transcripts per million are presented in Supplementary Table 20, as this unit allows efficient comparison of gene expression levels between samples from different studies.

Identifying overlap between NEB hits and previously identified selection signals

We assessed the overlap of our NEB signals with the results of three genome-wide selection scans: the Composite of Multiple Signals test[31], which combines information from different statistics to detect selection on the order of the past 50,000 years; an ancient-DNA-based scan[28] that uses direct inference of allele frequency from ancient populations to infer selection over the past 10,000 years; and the Singleton Density Score[29], which uses patterns of singleton variants to infer very recent selection, on the order of a few thousand years.

For the Composite of Multiple Signals test[31], we used the rankings of CMS_{GW} statistics to obtain an empirical P value for each SNP. For the Singleton Density Score[29], we converted normalized SDS scores to two-tailed P values of the standard normal distribution. Finally, for the ancient-DNA-based selection scan[28], we used the genomic control corrected P values from the original scan. For each NEB hit, for each scan, we identified the SNP within 10 kb, with $P < 10^{-6}$ for NEB that had the most significant selection scan signal (SNP1 and PVAL1 in Supplementary Tables 19 and 20). We also identified the SNP within 10 kb that had the most significant selection scan signal, regardless of its NEB P value (SNP2 and PVAL2 in Supplementary Tables 19 and 20). Finally, we performed a Bayesian colocalization analysis using the coloc package[32] using all SNPs within 10 kb of the lead NEB SNP. This computes posterior probabilities for the following hypotheses: H_0, no causal SNPs; H_1, causal SNP for selection but not for NEB; H_2, causal SNP for NEB but not for selection; H_3, one independent causal SNP for each trait; and H_4, one shared causal SNP for both traits. We report the hypothesis with the maximum posterior probability (COLOC in Supplementary Tables 19 and 20).

We also tested for overlap with a scan for balancing selection using the NCD2 statistic[44] for the GBR population of 1000 Genomes. We used the target frequency of 0.5 for these tests. For each SNP, we report the value of the window that overlaps that SNP, or, if more than one window overlaps a SNP, we report the lowest P value of any window within 10 kb. Finally, we report the lowest P value for genes within 10 kb of each SNP.

Estimating *FADS1* allele frequencies from ancient DNA

We downloaded combined data from https://reich.hms.harvard.edu/allen-ancient-dna-resource-aadr-downloadable-genotypes-present-day-and-ancient-dna-data (v.37.2, accessed 14 May 2019) and restricted them to 595 samples west of 40° E, north of 35° S, more recent than 12,000 years before the present and with coverage at rs108499. We binned them into 2,000-year bins and computed estimated allele frequencies and bootstrap CIs. We also included the European subpopulations from phase 3 of the 1000 Genomes Project[71].

Reporting summary

Further information on research design is available in the Nature Portfolio Reporting Summary linked to this article.

Data availability

Upon publication, the GWAS summary statistics will be made available at https://doi.org/10.17863/CAM.88397. Access to individual-level data from the multiple sources used in this GWAS can be obtained by bona fide scientists through application to each specific data provider; each data source is described in the Supplementary Note. Source data are provided with this paper.

Code availability

No custom code was used in this study. All analyses and modelling used standard software as described in the Methods and the Supplementary Information.

References

1. Day, F. R. et al. Causal mechanisms and balancing selection inferred from genetic associations with polycystic ovary syndrome. *Nat. Commun.* **6**, 8464 (2015).
2. Day, F. et al. Large-scale genome-wide meta-analysis of polycystic ovary syndrome suggests shared genetic architecture for different diagnosis criteria. *PLoS Genet.* **14**, e1007813 (2018).
3. Censin, J. C., Bovijn, J., Holmes, M. V. & Lindgren, C. M. Commentary: Mendelian randomization and women's health. *Int. J. Epidemiol.* **48**, 830–833 (2019).
4. O'Connor, L. J. et al. Extreme polygenicity of complex traits is explained by negative selection. *Am. J. Hum. Genet.* **105**, 456–476 (2019).
5. Weissbrod, O. et al. Functionally informed fine-mapping and polygenic localization of complex trait heritability. *Nat. Genet.* **52**, 1355–1363 (2020).
6. Balbo, N., Billari, F. C. & Mills, M. Fertility in advanced societies: a review of research. *Eur. J. Popul.* **29**, 1–38 (2013).
7. Mills, M., Rindfuss, R. R., McDonald, P. & te Velde, E. Why do people postpone parenthood? Reasons and social policy incentives. *Hum. Reprod. Update* **17**, 848–860 (2011).
8. Tropf, F. C. et al. Hidden heritability due to heterogeneity across seven populations. *Nat. Hum. Behav.* **1**, 757–765 (2017).
9. Day, F. R. et al. Physical and neurobehavioral determinants of reproductive onset and success. *Nat. Genet.* **48**, 617–623 (2016).
10. Barban, N. et al. Genome-wide analysis identifies 12 loci influencing human reproductive behavior. *Nat. Genet.* **48**, 1462–1472 (2016).
11. Mills, M. et al. Identification of 371 genetic variants for age at first sex and birth linked to externalising behaviour. *Nat. Hum. Behav.* **5**, 1717–1730 (2021).
12. Tropf, F. C. et al. Human fertility, molecular genetics, and natural selection in modern societies. *PLoS ONE* **10**, e0126821 (2015).
13. Day, F. R. et al. Genomic analyses identify hundreds of variants associated with age at menarche and support a role for puberty timing in cancer risk. *Nat. Genet.* **49**, 834–841 (2017).
14. Day, F. R. et al. Large-scale genomic analyses link reproductive aging to hypothalamic signaling, breast cancer susceptibility and BRCA1-mediated DNA repair. *Nat. Genet.* **47**, 1294–1303 (2015).
15. Kong, A. et al. Selection against variants in the genome associated with educational attainment. *Proc. Natl Acad. Sci. USA* **114**, E727–E732 (2017).
16. Beauchamp, J. P. Genetic evidence for natural selection in humans in the contemporary United States. *Proc. Natl Acad. Sci. USA* **113**, 7774–7779 (2016).
17. Bulik-Sullivan, B. K. et al. LD score regression distinguishes confounding from polygenicity in genome-wide association studies. *Nat. Genet.* **47**, 291–295 (2015).
18. Day, F. R., Ong, K. K. & Perry, J. R. B. Elucidating the genetic basis of social interaction and isolation. *Nat. Commun.* **9**, 2457 (2018).
19. Okbay, A. et al. Genome-wide association study identifies 74 loci associated with educational attainment. *Nature* **533**, 539–542 (2016).
20. Reddy, P. et al. Oocyte-specific deletion of Pten causes premature activation of the primordial follicle pool. *Science* **319**, 611–613 (2008).
21. de Leeuw, C. A., Mooij, J. M., Heskes, T. & Posthuma, D. MAGMA: generalized gene-set analysis of GWAS data. *PLoS Comput. Biol.* **11**, e1004219 (2015).
22. Morgan, M. D. et al. Genome-wide study of hair colour in UK Biobank explains most of the SNP heritability. *Nat. Commun.* **9**, 5271 (2018).
23. Hollis, B. et al. Genomic analysis of male puberty timing highlights shared genetic basis with hair colour and lifespan. *Nat. Commun.* **11**, 1536 (2020).
24. Bansal, S. K., Gupta, N., Sankhwar, S. N. & Rajender, S. Differential genes expression between fertile and infertile spermatozoa revealed by transcriptome analysis. *PLoS ONE* **10**, e0127007 (2015).
25. Thompson, D. J. et al. Genetic predisposition to mosaic Y chromosome loss in blood. *Nature* **575**, 652–657 (2019).
26. Nakamura, N. et al. Disruption of a spermatogenic cell-specific mouse enolase 4 (eno4) gene causes sperm structural defects and male infertility. *Biol. Reprod.* **88**, 90 (2013).
27. Ganna, A. et al. Large-scale GWAS reveals insights into the genetic architecture of same-sex sexual behavior. *Science* **365**, eaat7693 (2019).
28. Mathieson, I. et al. Genome-wide patterns of selection in 230 ancient Eurasians. *Nature* **528**, 499–503 (2015).
29. Field, Y. et al. Detection of human adaptation during the past 2000 years. *Science* **354**, 760–764 (2016).
30. Grossman, S. R. et al. A composite of multiple signals distinguishes causal variants in regions of positive selection. *Science* **327**, 883–886 (2010).
31. Grossman, S. R. et al. Identifying recent adaptations in large-scale genomic data. *Cell* **152**, 703–713 (2013).
32. Giambartolomei, C. et al. Bayesian test for colocalisation between pairs of genetic association studies using summary statistics. *PLoS Genet.* **10**, e1004383 (2014).
33. Fumagalli, M. et al. Greenlandic Inuit show genetic signatures of diet and climate adaptation. *Science* **349**, 1343–1347 (2015).
34. Ameur, A. et al. Genetic adaptation of fatty-acid metabolism: a human-specific haplotype increasing the biosynthesis of long-chain omega-3 and omega-6 fatty acids. *Am. J. Hum. Genet.* **90**, 809–820 (2012).
35. Ye, K., Gao, F., Wang, D., Bar-Yosef, O. & Keinan, A. Dietary adaptation of FADS genes in Europe varied across time and geography. *Nat. Ecol. Evol.* **1**, 167 (2017).
36. Buckley, M. T. et al. Selection in Europeans on fatty acid desaturases associated with dietary changes. *Mol. Biol. Evol.* **34**, 1307–1318 (2017).
37. Mathieson, S. & Mathieson, I. FADS1 and the timing of human adaptation to agriculture. *Mol. Biol. Evol.* **35**, 2957–2970 (2018).
38. Teslovich, T. M. et al. Biological, clinical and population relevance of 95 loci for blood lipids. *Nature* **466**, 707–713 (2010).
39. Draisma, H. H. M. et al. Genome-wide association study identifies novel genetic variants contributing to variation in blood metabolite levels. *Nat. Commun.* **6**, 7208 (2015).
40. Stoffel, W. et al. Dietary ω3-and ω6-polyunsaturated fatty acids reconstitute fertility of juvenile and adult Fads2-deficient mice. *Mol. Metab.* **36**, 100974 (2020).
41. Klarin, D. et al. Genetics of blood lipids among ~300,000 multi-ethnic participants of the Million Veteran Program. *Nat. Genet.* **50**, 1514–1523 (2018).

42. Siewert, K. M. & Voight, B. F. Detecting long-term balancing selection using allele frequency correlation. *Mol. Biol. Evol.* **34**, 2996–3005 (2017).

43. Boutwell, B. et al. Replication and characterization of CADM2 and MSRA genes on human behavior. *Heliyon* **3**, e00349 (2017).

44. Bitarello, B. D. et al. Signatures of long-term balancing selection in human genomes. *Genome Biol. Evol.* **10**, 939–955 (2018).

45. Fry, A. et al. Comparison of sociodemographic and health-related characteristics of UK Biobank participants with those of the general population. *Am. J. Epidemiol.* **186**, 1026–1034 (2017).

46. Wood, A. R. et al. Defining the role of common variation in the genomic and biological architecture of adult human height. *Nat. Genet.* **46**, 1173–1186 (2014).

47. van der Most, P. J. et al. QCGWAS: a flexible R package for automated quality control of genome-wide association results. *Bioinformatics* **30**, 1185–1186 (2014).

48. Winkler, T. W. et al. Quality control and conduct of genome-wide association meta-analyses. *Nat. Protoc.* **9**, 1192–1212 (2014).

49. Price, A. L. et al. Principal components analysis corrects for stratification in genome-wide association studies. *Nat. Genet.* **38**, 904–909 (2006).

50. Loh, P.-R. et al. Efficient Bayesian mixed-model analysis increases association power in large cohorts. *Nat. Genet.* **47**, 284–290 (2015).

51. Rietveld, C. A. et al. GWAS of 126,559 individuals identifies genetic variants associated with educational attainment. *Science* **340**, 1467–1471 (2013).

52. Willer, C. J., Li, Y. & Abecasis, G. R. METAL: fast and efficient meta-analysis of genomewide association scans. *Bioinformatics* **26**, 2190–2191 (2010).

53. Evangelou, E. & Ioannidis, J. P. A. Meta-analysis methods for genome-wide association studies and beyond. *Nat. Rev. Genet.* **14**, 379–389 (2013).

54. Yang, J., Lee, S. H., Goddard, M. E. & Visscher, P. M. GCTA: a tool for genome-wide complex trait analysis. *Am. J. Hum. Genet.* **88**, 76–82 (2011).

55. Yang, J. et al. Conditional and joint multiple-SNP analysis of GWAS summary statistics identifies additional variants influencing complex traits. *Nat. Genet.* **44**, 369–375 (2012).

56. Bulik-Sullivan, B. et al. An atlas of genetic correlations across human diseases and traits. *Nat. Genet.* **47**, 1236–1241 (2015).

57. Manichaikul, A. et al. Robust relationship inference in genome-wide association studies. *Bioinformatics* **26**, 2867–2873 (2010).

58. Chang, C. C. et al. Second-generation PLINK: rising to the challenge of larger and richer datasets. *GigaScience*, **4**, https://doi.org/10.1186/s13742-015-0047-8 (2015).

59. Zhu, Z. et al. Integration of summary data from GWAS and eQTL studies predicts complex trait gene targets. *Nat. Genet.* **48**, 481–487 (2016).

60. Võsa, U. et al. Large-scale *cis*- and *trans*-eQTL analyses identify thousands of genetic loci and polygenic scores that regulate blood gene expression. *Nat. Genet.* **53**, 1300–1310 (2021).

61. Finucane, H. K. et al. Heritability enrichment of specifically expressed genes identifies disease-relevant tissues and cell types. *Nat. Genet.* **50**, 621–629 (2018).

62. GTEx Consortium. The Genotype-Tissue Expression (GTEx) pilot analysis: multitissue gene regulation in humans. *Science* **348**, 648–660 (2015).

63. Backman, J. D. et al. Exome sequencing and analysis of 454,787 UK Biobank participants. *Nature* **599**, 628–634 (2021).

64. Ruth, K. S. et al. Using human genetics to understand the disease impacts of testosterone in men and women. *Nat. Med.* **26**, 252–258 (2020).

65. Li, L. et al. Single-cell RNA-seq analysis maps development of human germline cells and gonadal niche interactions. *Cell Stem Cell* **20**, 858–873.e4 (2017).

66. Zhang, Y. et al. Transcriptome landscape of human folliculogenesis reveals oocyte and granulosa cell interactions. *Mol. Cell* **72**, 1021–1034.e4 (2018).

67. Bolger, A. M., Lohse, M. & Usadel, B. Trimmomatic: a flexible trimmer for Illumina sequence data. *Bioinformatics* **30**, 2114–2120 (2014).

68. Chen, S. et al. AfterQC: automatic filtering, trimming, error removing and quality control for fastq data. *BMC Bioinf.* **18**, 80 (2017).

69. Pertea, M., Kim, D., Pertea, G. M., Leek, J. T. & Salzberg, S. L. Transcript-level expression analysis of RNA-seq experiments with HISAT, StringTie and Ballgown. *Nat. Protoc.* **11**, 1650–1667 (2016).

70. Li, H. et al. The Sequence Alignment/Map format and SAMtools. *Bioinformatics* **25**, 2078–2079 (2009).

71. The 1000 Genomes Project Consortium. A global reference for human genetic variation. *Nature* **526**, 68–74 (2015).

Acknowledgements

Author contributions

I.M., H.S., M.d.H., K.K.O., M.C.M. and J.R.B.P. designed the study. I.M., F.R.D., N.B., F.C.T., D.M.B., A.V., N.v.Z., B.D.B., E.J.G., M.d.H. and J.R.B.P. performed the analyses. All authors contributed to the data collection and curation and critically reviewed the manuscript.

Competing interests

Additional information

Iain Mathieson [1,86] ✉, Felix R. Day [2,86], Nicola Barban[3,86], Felix C. Tropf[4,5,6,86], David M. Brazel[4,7,86], eQTLGen Consortium*, BIOS Consortium*, Ahmad Vaez [8,9], Natalie van Zuydam[10], Bárbara D. Bitarello[1], Eugene J. Gardner [2], Evelina T. Akimova [4,7], Ajuna Azad[11], Sven Bergmann [12,13,14], Lawrence F. Bielak[15], Dorret I. Boomsma [16,17], Kristina Bosak[18], Marco Brumat[19], Julie E. Buring[20,21], David Cesarini[22,23,24], Daniel I. Chasman [20,21], Jorge E. Chavarro[25,26,27], Massimiliano Cocca [28], Maria Pina Concas [28], George Davey Smith [29], Gail Davies [30], Ian J. Deary[30], Tõnu Esko[31,32], Jessica D. Faul[33], FinnGen Study*, Oscar Franco [34,35], Andrea Ganna [36,37], Audrey J. Gaskins [38], Andrea Gelemanovic[39], Eco J. C. de Geus[16], Christian Gieger [40], Giorgia Girotto [19,28], Bamini Gopinath[41], Hans Jörgen Grabe [42], Erica P. Gunderson [43], Caroline Hayward[44], Chunyan He [45,46], Diana van Heemst[47], W. David Hill[30], Eva R. Hoffmann [11], Georg Homuth[48], Jouke Jan Hottenga[16], Hongyang Huang[25], Elina Hyppönen [49,50], M. Arfan Ikram [34], Rick Jansen[51], Magnus Johannesson [52], Zoha Kamali [8,9], Sharon L. R. Kardia[15], Maryam Kavousi [34], Annette Kifley [41], Tuomo Kiiskinen [36,53], Peter Kraft [25,54], Brigitte Kühnel[40], Claudia Langenberg [2], Gerald Liew[41], Lifelines Cohort Study*, Penelope A. Lind [55], Jian'an Luan [2], Reedik Mägi[31], Patrik K. E. Magnusson [56], Anubha Mahajan [57,58], Nicholas G. Martin[59], Hamdi Mbarek [16,60], Mark I. McCarthy[57,58], George McMahon[61], Sarah E. Medland[55], Thomas Meitinger[62], Andres Metspalu [31,63], Evelin Mihailov[31], Lili Milani [31], Stacey A. Missmer[25,64,65], Paul Mitchell[41], Stine Møllegaard [66], Dennis O. Mook-Kanamori[67,68], Anna Morgan [28], Peter J. van der Most [8], Renée de Mutsert[67], Matthias Nauck [69], Ilja M. Nolte [8], Raymond Noordam [47], Brenda W. J. H. Penninx[70], Annette Peters [71], Patricia A. Peyser[15], Ozren Polašek[39,72], Chris Power[73], Ajka Pribisalic [39], Paul Redmond[30], Janet W. Rich-Edwards[25,27,74], Paul M. Ridker[20,21], Cornelius A. Rietveld [75,76], Susan M. Ring [29], Lynda M. Rose[20], Rico Rueedi[12,13], Vallari Shukla[11], Jennifer A. Smith [15,33], Stasa Stankovic [2], Kári Stefánsson[77], Doris Stöckl[71], Konstantin Strauch[78,79,80], Morris A. Swertz[81], Alexander Teumer [82], Gudmar Thorleifsson[77], Unnur Thorsteinsdottir[77], A. Roy Thurik [75,76,83], Nicholas J. Timpson [29], Constance Turman[25], André G. Uitterlinden [75,84], Melanie Waldenberger [40,71], Nicholas J. Wareham [2], David R. Weir [33], Gonneke Willemsen[16], Jing Hau Zhao[2], Wei Zhao [15], Yajie Zhao [2], Harold Snieder [8], Marcel den Hoed [10], Ken K. Ong [2], Melinda C. Mills [4,7,81,85,86] ✉ & John R. B. Perry [2,86] ✉

[1]Department of Genetics, Perelman School of Medicine, University of Pennsylvania, Philadelphia, PA, USA. [2]MRC Epidemiology Unit, Institute of Metabolic Science, University of Cambridge, Cambridge, UK. [3]Alma Mater Studiorum University of Bologna, Bologna, Italy. [4]Nuffield College, University of Oxford, Oxford, UK. [5]École Nationale de la Statistique et de L'administration Économique (ENSAE), Paris, France. [6]Center for Research in Economics and Statistics (CREST), Paris, France. [7]Leverhulme Centre for Demographic Science, University of Oxford, Oxford, UK. [8]Department of Epidemiology, University of Groningen, University Medical Center Groningen, Groningen, the Netherlands. [9]Department of Bioinformatics, Isfahan University of Medical Sciences, Isfahan, Iran. [10]Beijer Laboratory and Department of Immunology, Genetics and Pathology, Uppsala University and SciLifeLab, Uppsala, Sweden. [11]DNRF Center for Chromosome Stability, Department of Cellular and Molecular Medicine, Faculty of Health and Medical Sciences, University of Copenhagen, Copenhagen, Denmark. [12]Department of Computational Biology, University of Lausanne, Lausanne, Switzerland. [13]Swiss Institute of Bioinformatics, Lausanne, Switzerland. [14]Department of Integrative Biomedical Sciences, University of Cape Town, Cape Town, South Africa. [15]Department of Epidemiology, University of Michigan, Ann Arbor, MI, USA. [16]Department of Biological Psychology, Amsterdam Public Health Research Institute, Vrije Universiteit Amsterdam, Amsterdam, the Netherlands. [17]Amsterdam Reproduction and Development (AR&D) Research Institute, Amsterdam, the Netherlands. [18]Psychiatric Hospital 'Sveti Ivan', Zagreb, Croatia. [19]Department of Medical, Surgical and Health Sciences, University of Trieste, Trieste, Italy. [20]Brigham and Women's Hospital, Boston, MA, USA. [21]Harvard Medical School, Boston, MA, USA. [22]Department of Economics, New York University, New York, NY, USA. [23]Research Institute for Industrial Economics, Stockholm, Sweden. [24]National Bureau of Economic Research, Cambridge, MA, USA. [25]Department of Epidemiology, Harvard T.H. Chan School of Public Health, Boston, MA, USA. [26]Department of Nutrition, Harvard T.H. Chan School of Public Health, Boston, MA, USA. [27]Channing Division of Network Medicine, Brigham and Women's Hospital and Harvard Medical School, Boston, MA, USA. [28]Institute for Maternal and Child Health, IRCCS 'Burlo Garofolo', Trieste, Italy. [29]MRC Integrative Epidemiology Unit, University of Bristol, Bristol, UK. [30]Lothian Birth Cohorts, Department of Psychology, University of Edinburgh, Edinburgh, UK. [31]Estonian Genome Center, University of Tartu, Tartu, Estonia. [32]Broad Institute of the Massachusetts Institute of Technology and Harvard University, Cambridge, MA, USA. [33]Survey Research Center, Institute for Social Research, University of Michigan, Ann Arbor, MI, USA. [34]Department of Epidemiology, Erasmus MC, University Medical Center Rotterdam, Rotterdam, the Netherlands. [35]Julius Center for Health Sciences and Primary Care, University Medical Center Utrecht, Utrecht University, Utrecht, the Netherlands. [36]Institute for Molecular Medicine Finland (FIMM), HiLIFE, University of Helsinki, Helsinki, Finland. [37]Analytic and Translational Genetics Unit, Center for Genomic Medicine, Massachusetts General Hospital, Boston, MA, USA. [38]Department of Epidemiology, Rollins School of Public Health, Emory University, Atlanta, GA, USA. [39]University of Split School of Medicine, Split, Croatia. [40]Research Unit of Molecular Epidemiology, Helmholtz Zentrum München,

German Research Center for Environmental Health, Neuherberg, Germany. [41]Centre for Vision Research, Westmead Institute for Medical Research and Department of Ophthalmology, University of Sydney, Sydney, New South Wales, Australia. [42]Department of Psychiatry and Psychotherapy, University Medicine Greifswald, Greifswald, Germany. [43]Division of Research, Kaiser Permanente Northern California, Oakland, CA, USA. [44]Medical Research Council Human Genetics Unit, Institute of Genetics and Cancer, University of Edinburgh, Edinburgh, UK. [45]Markey Cancer Center, University of Kentucky, Lexington, KY, USA. [46]Department of Internal Medicine, Division of Medical Oncology, University of Kentucky College of Medicine, Lexington, KY, USA. [47]Department of Internal Medicine, Section of Gerontology and Geriatrics, Leiden University Medical Center, Leiden, the Netherlands. [48]Interfaculty Institute for Genetics and Functional Genomics, University of Greifswald, Greifswald, Germany. [49]Australian Centre for Precision Health, University of South Australia Cancer Research Institute, Adelaide, South Australia, Australia. [50]South Australian Health and Medical Research Institute, Adelaide, South Australia, Australia. [51]Department of Psychiatry, Amsterdam Public Health and Amsterdam Neuroscience, Amsterdam UMC, Vrije Universiteit, Amsterdam, the Netherlands. [52]Department of Economics, Stockholm School of Economics, Stockholm, Sweden. [53]National Institute for Health and Welfare, Helsinki, Finland. [54]Department of Biostatistics, Harvard T.H. Chan School of Public Health, Boston, MA, USA. [55]Psychiatric Genetics, QIMR Berghofer Medical Research Institute, Brisbane, Queensland, Australia. [56]Department of Medical Epidemiology and Biostatistics, Karolinska Institutet, Stockholm, Sweden. [57]Wellcome Centre for Human Genetics, University of Oxford, Oxford, UK. [58]Oxford Centre for Diabetes, Endocrinology and Metabolism, Radcliffe Department of Medicine, University of Oxford, Oxford, UK. [59]Genetic Epidemiology, QIMR Berghofer Medical Research Institute, Brisbane, Queensland, Australia. [60]Qatar Genome Programme, Qatar Foundation Research, Development and Innovation, Qatar Foundation, Doha, Qatar. [61]School of Social and Community Medicine, University of Bristol, Bristol, UK. [62]Institute of Human Genetics, Helmholtz Zentrum München, German Research Center for Environmental Health, Neuherberg, Germany. [63]Institute of Molecular and Cell Biology, University of Tartu, Tartu, Estonia. [64]Division of Adolescent and Young Adult Medicine, Department of Medicine, Boston Children's Hospital and Harvard Medical School, Boston, MA, USA. [65]Department of Obstetrics, Gynecology, and Reproductive Biology, College of Human Medicine, Michigan State University, Grand Rapids, MI, USA. [66]Department of Sociology, University of Copenhagen, Copenhagen, Denmark. [67]Department of Clinical Epidemiology, Leiden University Medical Center, Leiden, the Netherlands. [68]Department of Public Health and Primary Care, Leiden University Medical Center, Leiden, the Netherlands. [69]Institute of Clinical Chemistry and Laboratory Medicine, University Medicine Greifswald, Greifswald, Germany. [70]Department of Psychiatry, EMGO Institute for Health and Care Research and Neuroscience Campus Amsterdam, VU University Medical Center/GGZ inGeest, Amsterdam, the Netherlands. [71]Institute of Epidemiology, Helmholtz Zentrum München, German Research Center for Environmental Health, Neuherberg, Germany. [72]Algebra University College, Zagreb, Croatia. [73]Population, Policy and Practice Research and Teaching Department, UCL Great Ormond Street Institute of Child Health, London, UK. [74]Division of Women's Health, Department of Medicine, Brigham and Women's Hospital and Harvard Medical School, Boston, MA, USA. [75]Erasmus University Rotterdam Institute for Behavior and Biology, Rotterdam, the Netherlands. [76]Department of Applied Economics, Erasmus School of Economics, Rotterdam, the Netherlands. [77]deCODE Genetics/Amgen Inc., Reykjavik, Iceland. [78]Institute of Medical Biostatistics, Epidemiology and Informatics (IMBEI), University Medical Center, Johannes Gutenberg University, Mainz, Germany. [79]Institute of Genetic Epidemiology, Helmholtz Zentrum München, German Research Center for Environmental Health, Neuherberg, Germany. [80]Chair of Genetic Epidemiology, IBE, Faculty of Medicine, LMU, Munich, Germany. [81]Department of Genetics, University of Groningen, University Medical Center Groningen, Groningen, the Netherlands. [82]Institute for Community Medicine, University Medicine Greifswald, Greifswald, Germany. [83]Montpellier Business School, Montpellier, France. [84]Department of Internal Medicine, Erasmus MC, University Medical Center Rotterdam, Rotterdam, the Netherlands. [85]Department of Economics, Econometrics and Finance, University of Groningen, Groningen, the Netherlands. [86]These authors contributed equally: Iain Mathieson, Felix R. Day, Nicola Barban, Felix C. Tropf, David M. Brazel, Melinda C. Mills, John R. B. Perry. *A full list of members and their affiliations appears in the Supplementary Information. ✉e-mail: mathi@pennmedicine.upenn.edu; melinda.mills@nuffield.ox.ac.uk; john.perry@mrc-epid.cam.ac.uk

eQTLGen Consortium

Dorret I. Boomsma[16,17], Tõnu Esko[31,32], Lili Milani[31], Matthias Nauck[69], Brenda W. J. H. Penninx[70] & Alexander Teumer[82]

BIOS Consortium

Dorret I. Boomsma[16,17], Jouke Jan Hottenga[16], Diana van Heemst[47], Rick Jansen[51] & André G. Uitterlinden[75,84]

FinnGen Study

Andrea Ganna[36,37] & Tuomo Kiiskinen[36,53]

Lifelines Cohort Study

Ilja M. Nolte[8], Peter J. van der Most[8] & Morris A. Swertz[81]